

Stress-Strain Behavior by a Simple Elasto-Plastic Theory for Anisotropic Granular Materials II (Application)

簡単な弾塑性理論による異方性のある粒状体の応力-歪特性 II (応用)

by Fumio TATSUOKA*

龍岡 文夫

3. Analyses of the Data of Triaxial Compression and Plane Strain Compression Tests.

Green and Readers^{(3)**} performed vertical and horizontal triaxial compression tests on cuboidal samples 3.3 in. high, 3.0 in. long and 2.3 in. wide. They also performed vertical and horizontal plane strain tests on the samples of the same dimensions (Fig. 4). In the vertical

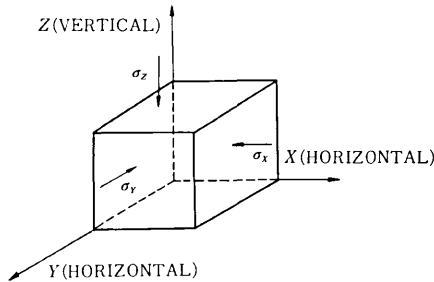


Fig. 4 A rectangular sample and the definitions of stresses

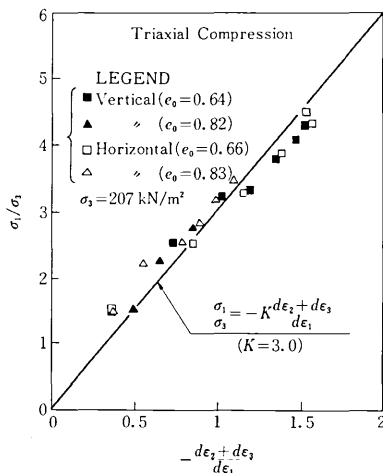


Fig. 5 Stress-dilatancy relations from triaxial compression tests by Green and Reads (1975)

* Dept. of Building and Civil Engineering.

** References are listed in the previous paper (Tatsuoka, F. (1978), "Stress-strain behavior by a simple elasto-plastic theory for anisotropic granular materials I (theory)," Seisan Kenkyu, Vol. 30, No. 7).

triaxial compression tests the direction of the major principal stress is vertical (z-direction in Fig. 4) and in the horizontal tests that is horizontal (x or y-direction in Fig. 4). It is reported that both loose and tamped dense samples were essentially isotropic with respect to strength, but were more compressible in the horizontal direction (Fig. 7).

From the theory, the stress-dilatancy equation both for the vertical triaxial compression tests (VTC) and for the horizontal compression tests (HTC) can be derived as⁽¹⁷⁾

$$\sigma_1/\sigma_3 = -K(d\epsilon_2 + d\epsilon_3)/d\epsilon_1 \quad (15)$$

Note that generally in the horizontal triaxial compression tests, $d\epsilon_2 \approx d\epsilon_3$. Fig. 5 shows that $K=3.0$ is appropriate

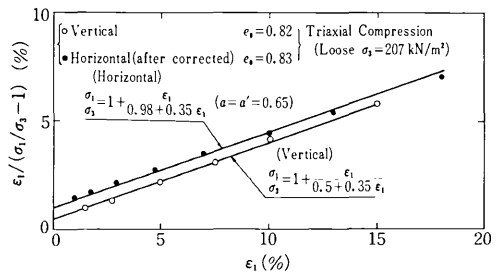


Fig. 6 Hyperbolic stress-strain relationships from the data by Green and Reads (1975)

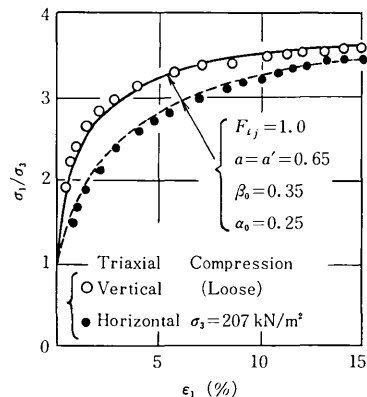


Fig. 7 Effects of inherent anisotropy on the stress-strain relationships by Green and Reads (1975) and theoretical curves

研究速報

both for VTC and HTC. Fig. 6 shows that the hyperbolic functions can be applicable to both VTC and HTC. These are $\sigma_1/\sigma_3 = 1 + \epsilon_1/(0.5 + 0.35\epsilon_1)$ for VTC (16) $\sigma_1/\sigma_3 = 1 + \epsilon_1/(0.98 + 0.35\epsilon_1)$ for HTC

The solid curves in Fig. 7 represent Equation (16). Note that the parameter α_{ij} is different between two equations. From Equations (5) and (16), for VTC in which $\sigma_z > \sigma_x = \sigma_y$

$$\begin{aligned} \epsilon_{zxx} &= \epsilon_{zzy} = \alpha_{zx}/((1/\sigma_z/\sigma_x - 1) - \beta_{zx}) \\ &= \alpha_{zy}/((\sigma_z/\sigma_y - 1) - \beta_{zy}) = \epsilon_z/2 \\ &= \epsilon_1/2 = 0.5/2/((1/\sigma_1/\sigma_3 - 1) - 0.35) \end{aligned} \quad (17)$$

Therefore, $\alpha_{zx} = \alpha_{zy} = \alpha_0 = 0.25$ and $\beta_{zx} = \beta_{zy} = \beta_0 = 0.35$ and for HTC in which $\sigma_x > \sigma_z = \sigma_y$

$$\begin{aligned} \epsilon_{xzx} + \epsilon_{xyx} &= \alpha_{xz}/((1/\sigma_x/\sigma_z - 1) - \beta_{zx}) \\ &\quad + \alpha_{xy}/((\sigma_x/\sigma_y - 1) - \beta_{xy}) \\ &= \epsilon_x = \epsilon_1 = 0.98/((1/\sigma_1/\sigma_3 - 1) - 0.35) \end{aligned} \quad (18)$$

When $\beta_{zx} = \beta_{xy} = \beta_0 = 0.35$ is assumed,

$$\alpha_{zx} + \alpha_{xy} = 0.98 \quad (19)$$

Here the parameters representing inherent anisotropy a and a' can be defined as

$$a = \alpha_{zx}/\alpha_{yx} = \alpha_{zy}/\alpha_{xy}, \quad a' = \alpha_{yx}/\alpha_{zy} = \alpha_{xy}/\alpha_{zx} \quad (20)$$

Note that $\alpha_{zx} = \alpha_{zy}$, $\alpha_{yx} = \alpha_{xy}$, $\alpha_{yz} = \alpha_{xy}$ and $\alpha_{yz} = \alpha_{xz}$. If $a = a'$ is assumed, the values of a and a' can be obtained from Equations (17), (19) and (20) as

$$a = a' = 0.65 \quad (21)$$

The measured values of b for the vertical plane strain test (VPS) and for the horizontal plane strain test (HPS) by Green and Reades⁽³⁾ are shown in Fig. 8. It can be noted that the values of b for HPS are considerably larger than those for VPS. This difference should be explained by inherent anisotropy of the samples tested. The theoretical

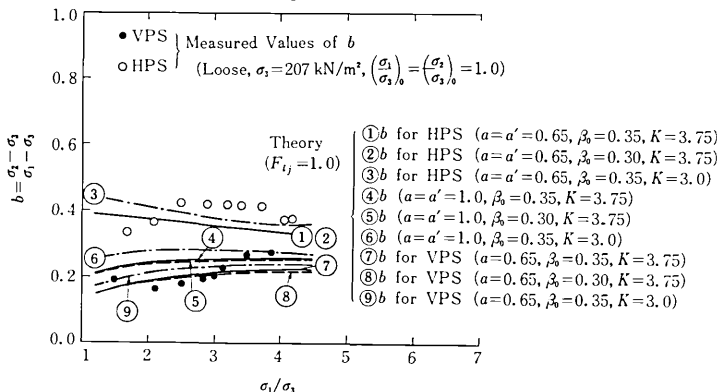


Fig. 8 Effects inherent anisotropy on the intermediate principal stress in the plane strain tests by Green and Reades and theoretical curves

curves for the b -values in Fig. 8 were obtained as follows. The intermediate principal strain increment $d\epsilon_2$ is derived by the theory as

$$d\epsilon_2 = d\epsilon_{212} + d\epsilon_{223} \quad (22)$$

From Equations (6), (7), (8), (9), (10), (11) and (22),

$$\begin{aligned} d\epsilon_2 &= -1/K \cdot \sigma_1/\sigma_2 \cdot \alpha_{12}/(1 - \beta_{12}(\sigma_1/\sigma_2 - 1) \\ &\quad - 1))^2 \cdot d(\sigma_1/\sigma_2) \\ &\quad + \alpha_{23}/(1 - \beta_{23}(\sigma_2/\sigma_3 - 1))^2 \cdot d(\sigma_2/\sigma_3) = 0 \end{aligned} \quad (23)$$

On the other hand,

$$\begin{aligned} d(\sigma_1/\sigma_2) &= 1/(\sigma_2/\sigma_3) \cdot d(\sigma_1/\sigma_3) \\ &\quad - (\sigma_1/\sigma_3)/(\sigma_2/\sigma_3)^2 \cdot d(\sigma_2/\sigma_3) \end{aligned} \quad (24)$$

From Equations (23), (24),

$$d(\sigma_2/\sigma_3) = \frac{\sigma_1/\sigma_3}{\left[\frac{((\sigma_1/\sigma_2)/(\sigma_2/\sigma_3))^2}{+ K(\alpha_{23}/\alpha_{12}) \cdot (1 - \beta_{12})} \cdot (\sigma_1/\sigma_2 - 1) / (1 - \beta_{23}) \cdot (\sigma_2/\sigma_3 - 1) \right]^2} \cdot d(\sigma_1/\sigma_3) \quad (25)$$

For VPS, $\alpha_{23}/\alpha_{12} = \alpha_{xy}/\alpha_{zy} = 1/a$ and $\beta_{12} = \beta_{zx} = \beta_{23} = \beta_{xy} = \beta_0$.

And for HPS, $\alpha_{23}/\alpha_{12} = \alpha_{zy}/\alpha_{xz} = a \cdot a'$ and $\beta_{12} = \beta_{zx} = \beta_{23} = \beta_{zy} = \beta_0$.

By the numerical integration using Equation (25), the relationship between σ_2/σ_3 and σ_1/σ_3 can be obtained. With the step of $d(\sigma_1/\sigma_3) = 0.2$ and with the initial values of $(\sigma_1/\sigma_3)_0 = (\sigma_2/\sigma_3)_0 = 1.0$, which correspond to the test conditions employed by Green and Reades, several theoretical curves of the relationships

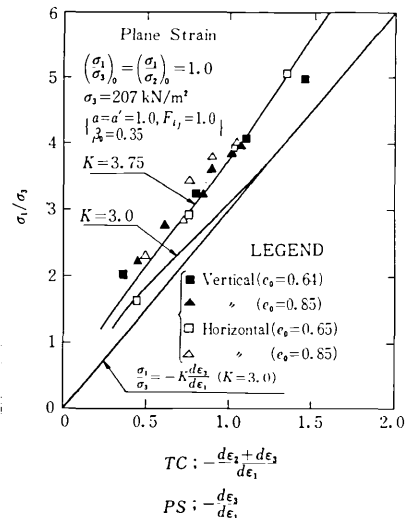


Fig. 9 Stress-dilatancy relationships of the plane strain tests by Green and Reades (1975) and theoretical curves

研究速報
 between $b = (\sigma_2 - \sigma_3) / (\sigma_1 - \sigma_3)$ and σ_1 / σ_3 were calculated for the several combinations of a , a' , β_0 and K . These theoretical curves are presented in Fig. 8. For $K = 3.0$, $a = a' = 0.65$ and $\beta_0 = 0.35$, the curve 3 should be compared with the b-value for HPS and the curve 9 should be compared with the b-value for VPS. Note that for the isotropic material of $a = a' = 1.0$, both curves 3 and 9 become the same one (the curve 6). It may be seen that the difference of the b-value between VPS and HPS can be seen between the two theoretical curves 3 and 9. The theoretical curves for $K = 3.75$, $a = a' = 0.65$ and $\beta_0 = 0.30$ and 0.35 for VPS are the curves 7 and 8. It may be seen that the effects of β_0 on the theoretical value are relatively small and that even for $K = 3.75$, $a = a' = 0.65$ and $\beta_0 = 0.30$ or 0.35 the theoretical values of b can be compared well with the measured values both for VPS and HPS.

The theoretical relationship between σ_1 / σ_3 and $d\varepsilon_3 / d\varepsilon_1$ for the plane strain tests can also be derived and compared with the data in Fig. 9. For the vertical plane strain tests (VPS), $\alpha_{13} / \alpha_{12} = \alpha_{zy} / \alpha_{zx} = 1.0$ and $\beta_{12} = \beta_{zx} = \beta_{13} = \beta_{zy} = \beta_0$ and for the horizontal plane test (HPS), $\alpha_{13} / \alpha_{12} = \alpha_{xy} / \alpha_{xz} = a'$ and $\beta_{12} = \beta_{zx} = \beta_{13} = \beta_{xy} = \beta_0$ in this case (Generally, $\beta_{zx} \neq \beta_{xy} \neq \beta_0$ can be possible).

As it was found that the effects of the values of a' and β_0 on the theoretical relationship are negligible for the range of $a = a' = 0.65 \sim 1.0$ and $\beta = 0.30 \sim 0.35$, only the curves for $a = a' = 1.0$ and $\beta_0 = 0.35$ and for $K = 3.0$ and 3.75 are presented and compared with the measured values as in Fig. 9. It is obvious that $K = 3.75$ is more appropriate than $K = 3.0$. This means that, following the theory presented, K should be considered to be affected by the b-value, with K being larger for $0 < b < 1$ than for $b = 0$ or 1 .

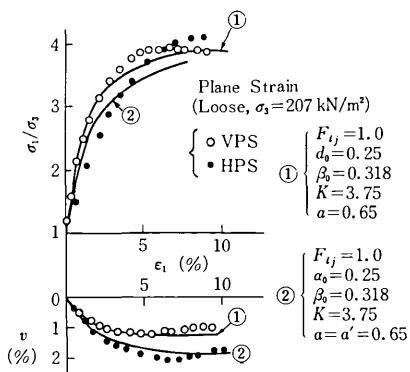


Fig. 10 Effects of inherent anisotropy on the stress-strain relationships of the plane strain tests by Green and Reades (1975) and theoretical curves

The theoretical relationships among σ_1 / σ_3 , ε_1 and v both for VPS and HPS were derived and compare with the measured values as in Fig. 10. In this procedure, it was found that $\beta_0 = 0.30$ is too small for fitting the theoretical curve to the measured values and $\beta_0 = 0.318$ was employed. The difference between two theoretical curves is due to the difference of α_{ij} . For VPS, $\alpha_{zx} = \alpha_{zy} = \alpha_0 = 0.25$, but for HPS $\alpha_{zx} = \alpha_0 / a \cdot a'$ and $\alpha_{zy} = \alpha_0 / a$. It can be seen from Fig. 10 that the difference of the stress-strain relationships between VPS and HPS can be duplicated by the theory adopting the proper anisotropic parameters a and a' .

4. Induced Anisotropy by the Theory

To simply describe the induced anisotropy by the theory, an idealized inherently isotropic material was assumed. This material has $K = 3.5$, $F_{ij} = 1.0$, $\alpha_{ij} = 0.3$ $\beta_{ij} = 0.3$ with these values being not affected by the b value and the direction of σ_1 . And each yield function f_{ij} is assumed to be independent of the others. Thus, the yielding and hardening properties of each idealized two dimensional slipping are assumed to be independent of the others. The yield loci on the $\sigma_x + \sigma_y + \sigma_z = \text{constant}$ plane are shown in Fig. 11 for $\sigma_i / \sigma_j = 2, 4$ and 6 . The angle θ is defined as the value from the σ_z -axis as shown in Fig. 11. Assume that this material is firstly sheared at $\theta = 0^\circ$ where $\sigma_1 = \sigma_z$ and $\sigma_2 = \sigma_3 = \sigma_x$ up to $R = \sigma_1 / \sigma_3 = 3.0$, then reloaded to $R = 0.0$. The stress-strain relationships during this procedure are shown in Fig. 12. Note that at the stress point C after loading and reloading of $A \rightarrow B \rightarrow C$, $f_{zx} = f_{zy} = 3.0$ and the other yield functions f_{ij} are 0.0. Then assume that this material

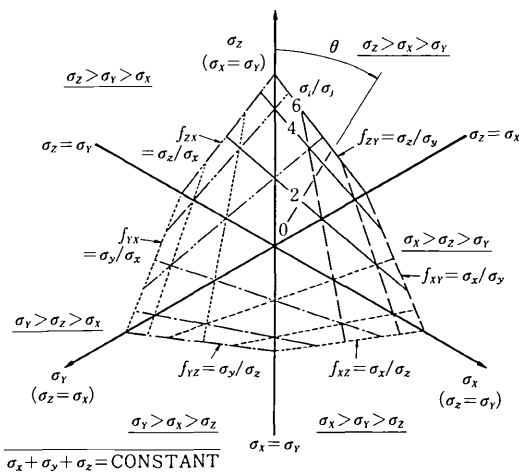


Fig. 11 The yield loci on the $\sigma_x + \sigma_y + \sigma_z = \text{constant}$ plane of the theory in the case of $F_{ij} = 1.0$

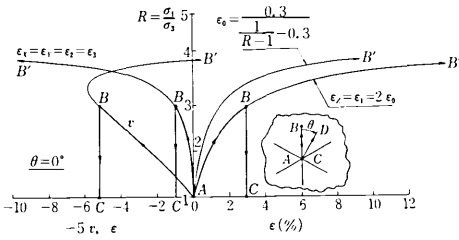


Fig. 12 Stress-strain relationships at first loading at $\theta = 0^\circ$

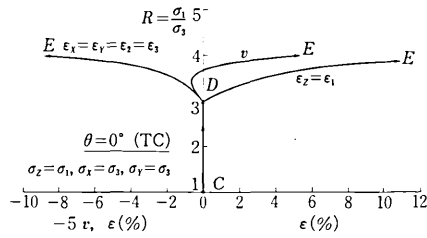


Fig. 13 Stress-strain relationship at reloading at $\theta = 0^\circ$

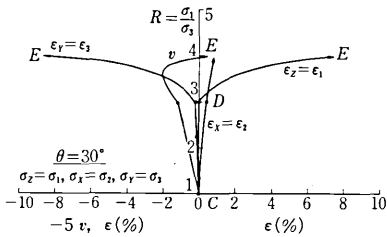


Fig. 14 Stress-strain relationship at reloading at $\theta = 30^\circ$

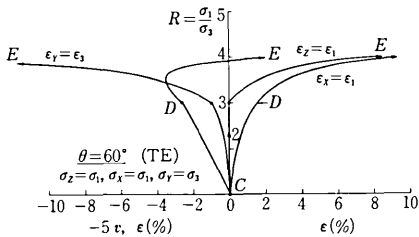


Fig. 15 Stress-strain relationship at reloading at $\theta = 60^\circ$

is reloaded as $C \rightarrow D \rightarrow E$ at the various values of θ ; 0° , 30° , 60° , 90° , 120° , 150° and 180° . The calculated stress-strain relationships for various values of θ are presented in Figs. 13 through 19. It can be seen from these figures that the response at reloading is considerably affected by the value of θ . Note that the deformability increases with increasing θ . And it was found that the effects of the first loading at $\theta = 0^\circ$ remain by $\theta = 90^\circ$ but the stress-strain relationships at $\theta = 120^\circ$, 150° and 180° are same with that of the virgin sample which does not have the stress history of $A \rightarrow B \rightarrow C$. It may be seen from the above that the anisotropy induced by the stress system can be modeled

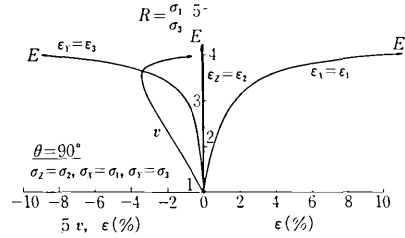


Fig. 16 Stress-strain relationship at reloading at $\theta = 90^\circ$

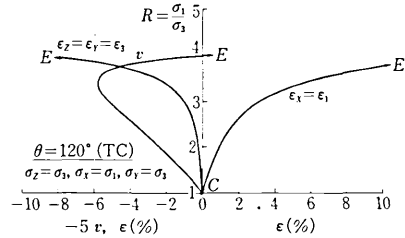


Fig. 17 Stress-strain relationship at reloading at $\theta = 120^\circ$

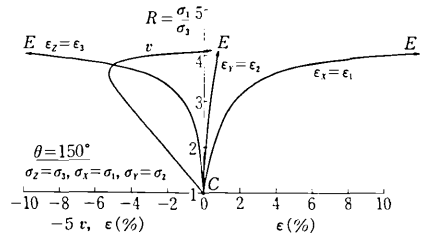


Fig. 18 Stress-strain relationship at reloading at $\theta = 150^\circ$

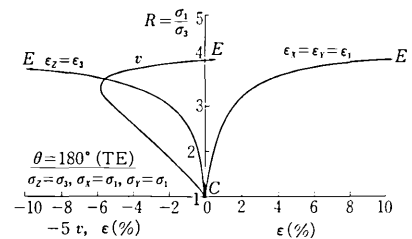


Fig. 19 Stress-strain relationship at reloading at $\theta = 180^\circ$

by this theory. But it is necessary to modify this theory based on the experimental data.

5. Conclusions

An elasto-plastic theory incorporating the anisotropic yield functions, the plastic potential functions and the empirical hardening functions which involve the parameters expressing inherent anisotropy has been presented. This theory is based on the postulate where actual principal strains are results of linear summation of two strain components in the idealized two dimensional slippings proposed by Matsuoka⁽⁵⁾. It was found that the inherent anisotropy and the stress-system induced anisotropy can be modeled by this theory. (Manuscript received, April 13, 1978)